Separation Science and Technology
Publication details, including instructions for authors and subscription information:
http://www.informaworld.com/smpp/title~content=t713708471

Transport and Permeation Properties of a Ternary Gas Mixture in a Medium-Size Polysulfone Hollow Fiber Permeator

Hisham M. Ettouney[a]; Osman Majeed[a]
[a] DEPARTMENT OF CHEMICAL ENGINEERING, KUWAIT UNIVERSITY, SAFAT, KUWAIT

To cite this Article Ettouney, Hisham M. and Majeed, Osman(1996) 'Transport and Permeation Properties of a Ternary Gas Mixture in a Medium-Size Polysulfone Hollow Fiber Permeator', Separation Science and Technology, 31: 11, 1573 — 1596
To link to this Article: DOI: 10.1080/01496399608001414
URL: http://dx.doi.org/10.1080/01496399608001414

SEPARATION SCIENCE AND TECHNOLOGY, 31(11), pp. 1573–1596, 1996

Transport and Permeation Properties of a Ternary Gas Mixture in a Medium-Size Polysulfone Hollow Fiber Permeator

HISHAM M. ETTOUNEY* and OSMAN MAJEED
DEPARTMENT OF CHEMICAL ENGINEERING
KUWAIT UNIVERSITY
PO BOX 5969, SAFAT 13060, KUWAIT

ABSTRACT

Permeation properties were analyzed for a mixture of CO_2, O_2, and N_2 in a medium-size polysulfone hollow fiber permeator with a net permeation area of 4.22 m^2. Measurements were conducted as a function of feed composition, reject flow rate, and feed pressure. Results included variations in species permeability, separation factor, permeate enrichment, reject depletion, and stage cut as a function of system parameters. Variations in permeation properties show strong dependence on feed composition, reject flow rate, and feed pressure. Permeability of carbon dioxide was higher at larger feed pressures and higher carbon dioxide content in the feed stream. Effect of increasing the reject flow rates on the permeability of carbon dioxide was affected by the system pressure and the carbon dioxide content in the feed stream. At low pressures, increase of the reject flow rate resulted in a decrease of carbon dioxide permeability. The opposite behavior was obtained at higher feed pressures. Increase of the reject flow rate reduced the gas residence time within the permeator. Increase of reject flow rate reduced species residence within the permeator and in turn increased resistance to species transport within the permeator. However, higher system pressures and carbon dioxide content in the feed stream resulted in larger levels of membrane plasticization, which increased the permeation rates of all species. The combined effect of reducing the species residence time within the permeator and the level of membrane plasticization favored the permeation of carbon dioxide versus the other two species. Variations in other permeation properties, which include oxygen and nitrogen permeabilities, stage cut, permeate enrichment in carbon dioxide, and reject depletion in carbon dioxide, were also explained in terms of resistances encountered within the permeator and the membrane.

* To whom correspondence should be addressed.

INTRODUCTION

Gaseous solubility and diffusivity in nonporous polymeric membranes are used as a measure for gaseous permeability through the membrane. In glassy polymers the dual mode model is commonly used to describe the solution process (1, 2). In the dual mode model, gaseous solubility is defined in terms of Henry's law solubility and Langmuir adsorption. The second part of the model involves a definition of gaseous diffusion in terms of mobility of dissolved and adsorbed species. More complex diffusion models involve interactions between both types of mobility (1, 2).

The above characteristics for gas permeation through glassy membranes were derived from data analysis for pure gases and from measurements for mixture gases. Data analysis shows that competition for adsorption sites in binary mixtures between low and fast permeating species causes a reduction in the permeability of the fast permeating species and enhances the permeability of the slow permeating species.

A large number of permeability studies for pure and binary mixtures can be found in the literature. The comprehensive reviews by Koros and Chern (1) and Zolandz and Fleming (2) cover a large number of these studies for a wide range of membrane materials, including silicon rubber, cellulose acetate, polycarbonate, polysulfone, etc., and for gases common to separation processes, including oxygen, nitrogen, hydrogen, methane, carbon dioxide, helium, etc.

One of the major aspects of studies on permeability measurements, e.g., Stern et al. (3), Li et al. (4), Donohue et al. (5), and Sada et al. (6), focused on comparison of pure gas permeability versus that in binary mixtures. Results in these studies show that permeability of the fast permeating species is lower in the mixture state than in the pure state. The opposite behavior was reported for the slow permeating species where higher permeabilities were measured in the mixture gas than in the pure gas. This behavior was attributed to membrane plasticization caused by the fast permeating species, which resulted in an increase of the void or hole volume within the membrane. This in turn improved the diffusion rates within the polymer chains and enhanced the permeation rates of the less permeable species. Higher degrees of plasticization occur at higher system pressures and result in lower selectivity and higher permeation flux.

Methods of membrane preparation also affect the characteristics of membrane separation. Techniques used to control membrane properties include modifications induced by substitute groups (7–9), polymer blending (10–13), and surface treatment through physical or chemical reactions (14–16). Substitute groups (7–9) alter the polymer glass transition temperature and in turn affect flexibility and relative motion of the polymer chains. Bulky groups are thought to reduce chain flexibility and to cause

an increase in the void or hole volume. These effects in turn can be induced to control membrane selectivity and species permeability.

Preparation of membranes through the use of polymer blends (10–13) was motivated by the fact that a polymer blend may possess separation properties superior to its pure constituents. Irrespective of this, the blend properties in some cases varied linearly with its composition (13).

Surface treatment (14–16) is the oldest technique used to alter separation properties of the membrane. Studies of this technique focused on comparison of separation properties for homogeneous dense membranes versus those of asymmetric or surface-treated membranes. Surface treatment may involve coating of a dense porous layer of a polymer membrane, e.g., cellulose acetate, with a thin layer of nonporous material, e.g., silicon rubber. Other treatment techniques were induced by nonsolvent solutions which may cause attraction or repulsion of polymer chains forming the membrane surface. In turn, this effect alters selectivity of the surface layer and species permeability.

Studies of surface treatment show that the skin layer in an asymmetric membrane may have a lower free volume ratio than in an isotropic membrane. In turn, this reduces the level of membrane plasticization and, as a result, the skin layer in an asymmetric membrane may possess higher selectivity than the dense layer (14). This result was reported by Pfromm et al. (14) for several types of membrane materials including polysulfone, polycarbonate, and poly(ester carbonate). However, opposite results were reported in a previous study by Sada et al. (15) on permeation of carbon dioxide through homogeneous dense and asymmetric cellulose acetate membranes. Their analysis show that in the asymmetric membranes the skin layer behaved in a similar manner to the dense layer, and its effect was limited to an increase of permeation resistance.

Permeation properties in a medium-size polysulfone permeator for a ternary gas mixture with fast, medium, and slow permeating species are the focus of this study. The gas mixture considered in the measurements includes CO_2, O_2, and N_2. The fast permeating species among the three gases is CO_2, followed by O_2 and then N_2. The above combination was selected to provide data on competitive effects among the three species on permeation properties. In addition, effects of permeator size on the transport properties of permeating species were analyzed as a function of system parameters, including reject flow rate, feed pressure, and feed composition.

PERMEATION SYSTEM AND MEASUREMENTS

The permeation system included two modules of asymmetric polysulfone hollow fiber membrane. The total membrane area provided by the

two modules was 4.22 m^2. The hollow fiber modules were tested with pressures up to 200 psig.

A schematic diagram of the system is shown in Fig. 1. As is shown, the two modules were arranged in a parallel configuration. The feed gas was introduced inside the fibers, and permeation takes place from the tube side to the shell side. As a result of the small diameter of the fibers, pressure drop inside the fibers was high; the measured pressure for the reject stream was 0 psig for all experimental conditions considered in the analysis.

The pressure of the feed stream was controlled by a regulator valve which operated over the 0–200 psig (0–1378 kPa) range. The maximum operating pressure used in the experiments was 150 psig (1034 kPa). The flow rates of the reject and permeate streams were measured by digital flowmeters which were calibrated with pure nitrogen gas at 0 psig and 298 K. Accordingly, measured flow rates were corrected using the measured room temperature, which varied from 22 to 25°C, and the average molecular weight of the reject and permeate streams, which was determined by using the compositions of both streams.

Mixtures of the feed gas were provided in high pressure cylinders through a local gas company. The composition of the cylinders was examined before conducting the experiments. Gas analysis was performed by

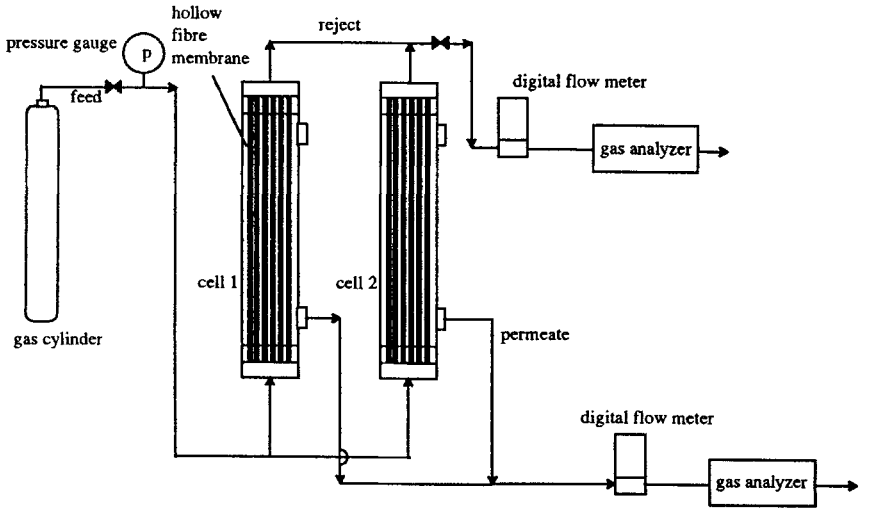

FIG. 1 Schematic of a two-stage hollow fiber gas separation system.

an infrared gas analyzer for CO_2 and an oxygen gas analyzer. Both analyzers were originally calibrated for mixtures containing CO_2, O_2, and N_2.

Start-up of the measurements required stabilization of the digital flowmeters and the gas analyzers. The stabilization time was 15 minutes with no gas flow into the system. During this period the flowmeters rapidly adjust to zero readings. Similarly, the CO_2 and O_2 analyzers were adjusted to concentration values of the ambient air. Gas analyzers provided continuous on-line measurements with the option of average measurements over a period of 1–4 minutes.

Measurements proceeded at the lowest pressure value, 207 kPa (30 psig). Instruments were allowed to adjust over a period of 10 minutes which was followed by measurements of compositions and flow rates of permeate and reject streams. Pressure was increased in steps to its highest value with simultaneous measurements of gas composition and flow rates at each pressure level. As the highest pressure (150 psig or 1378 kPa) was reached, the measurements were reversed by reducing the system pressure toward the lower end of the pressure scale. These measurements were performed to examine the level of membrane hysteresis. In addition, all measurements were repeated over a period 2 months to insure reproducibility of results.

PERMEABILITY MODEL AND PERMEATION CHARACTERISTICS

Species permeability was defined in terms of the permeate flow rate and the difference in the species partial pressures across the membrane. A linearized crossflow model was used to define the species permeability. The model assumed linear profiles for pressure and species concentrations in the tube side and uniform pressure and species concentrations in the shell side. Accordingly, the permeation rate of species i was defined as

$$y_i Q_p = R_i(\overline{P}_1 \overline{x}_i - P_2 y_i) \tag{1}$$

where

$$\overline{P}_1 = (P_1 + P_r)/2$$

and

$$\overline{x}_i = (Q_f x_f + Q_r x_r)/(Q_f + Q_r)$$

Equation (1) was rearranged to obtain the following expression for permeability of species i:

$$R_i = y_i Q_p/(A(\overline{P}_1 \overline{x}_i - P_2 y_i)) \tag{2}$$

From the above, determination of species permeability required definition of the total permeation area and measurements of

Species concentrations in feed, reject, and permeate streams
Pressures in feed and permeate compartments
Total permeate flow rate

Permeation characteristics were determined in terms of stage cut, reject depletion, and permeate enrichment. Stage cut was defined as the ratio of permeate flow rate to feed flow rate:

$$\text{Stage cut} = Q_p/Q_f$$

Permeate enrichment and reject depletion were defined as the ratio of the mole fraction of carbon dioxide in the permeate or reject streams to its mole fraction in the feed stream, i.e.,

$$\text{Permeate enrichment} = y_{CO_2}/x_{CO_{2f}}$$

and

$$\text{Reject depletion} = x_{CO_{2r}}/x_{CO_{2f}}$$

RESULTS AND DISCUSSION

Permeability measurements were made for a ternary mixture of CO_2, O_2, and N_2. The measurements were conducted as a function of feed composition, feed pressure, and reject flow rate. The two feed compositions used in the experiments had the following molar compositions:

5% CO_2, 25% O_2, and 70% N_2
10% CO_2, 20% O_2, and 70% N_2

Feed pressure was varied over a range of 206–1034 kPa and the reject flow rate was varied from 2–5 $L \cdot min^{-1}$. Data analysis included calculations of components permeability, separation factors, stage cut, reject depletion, and permeate enrichment.

Variations in CO_2 permeability versus feed pressure and as a function of reject flow rate and feed composition are shown in Figs. 2a, 2b, and 2c. Figures 2a and 2b show that CO_2 permeability increases over a range of 1×10^{-6} to 4×10^{-6} $m^3 \cdot m^{-2} \cdot s^{-1} \cdot kPa^{-1}$ as the system pressure is increased from 206 to 1034 kPa.

Increase of CO_2 permeability with pressure rise is associated with higher levels of membrane plasticization, which are caused primarily by CO_2. Increase in the level of membrane plasticization with pressure rise is a result of driving larger amount of CO_2 moles through the membrane. Ac-

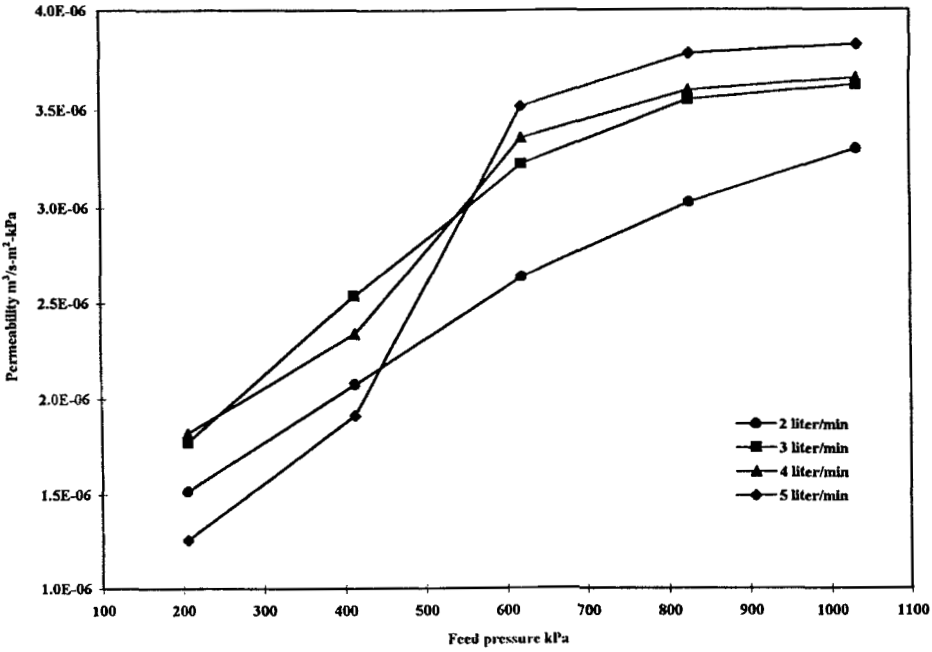

FIG. 2a Variation in CO_2 permeability as a function of feed pressure and reject flow rate with a feed composition of 5% CO_2, 25% O_2, and 70% N_2.

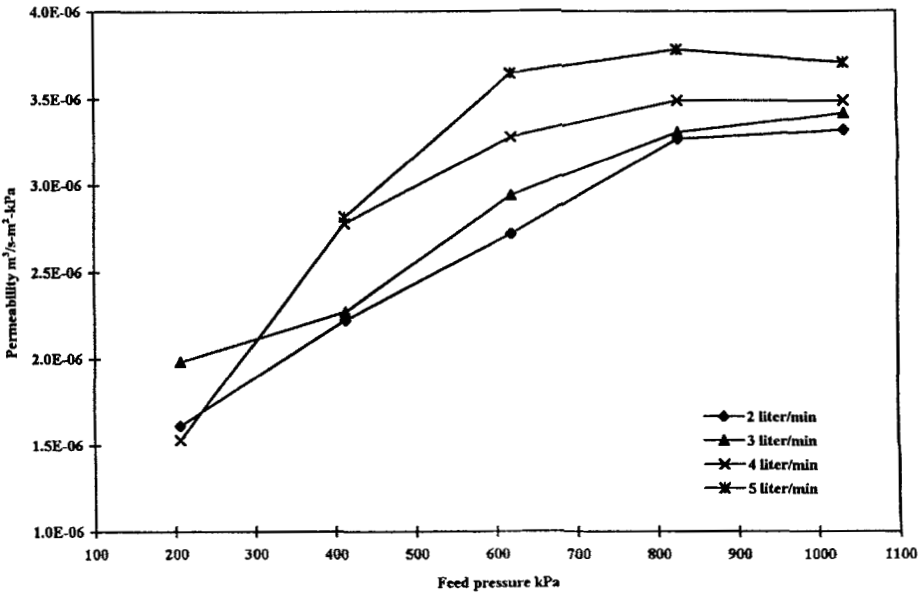

FIG. 2b Variation in CO_2 permeability as a function of feed pressure and reject flow rate with a feed composition of 10% CO_2, 20% O_2, and 70% N_2.

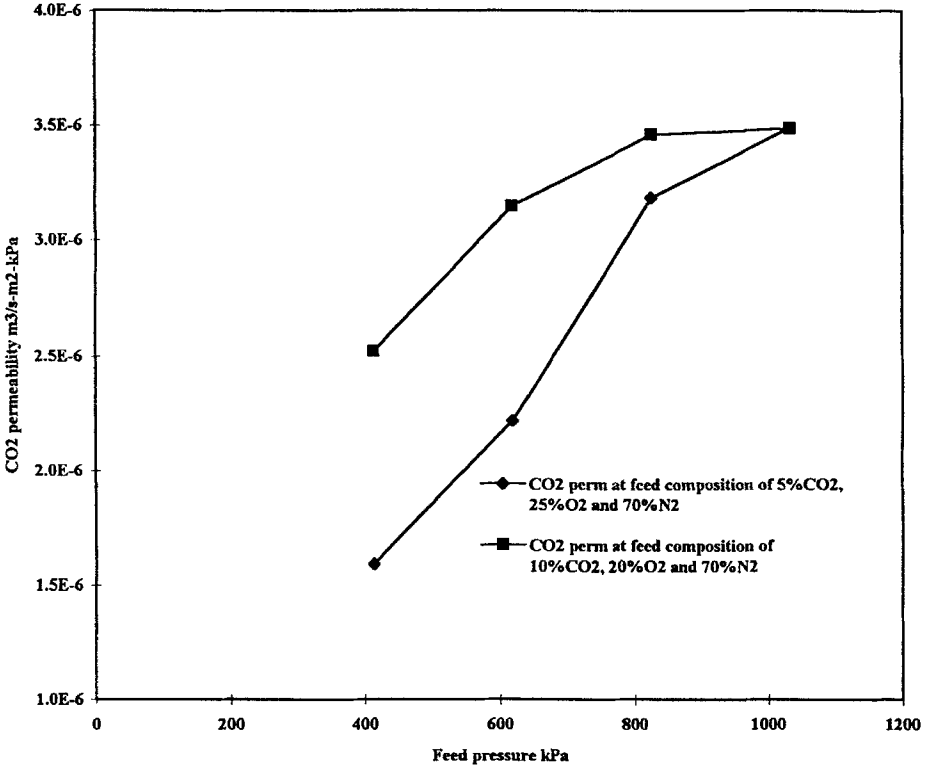

FIG. 2c Variation in average CO_2 permeability as a function of feed pressure and CO_2 feed composition.

cordingly, the hole or void volume within the membrane increases which enhances CO_2 permeability across the membrane.

Higher reject flow rates result in lowering the residence time for the feed mixture within the permeator. At lower residence times, higher resistance is realized for species transport within the system. As for CO_2, the combined effect of transport resistance and membrane plasticization favors its permeation across the membrane versus other species.

Averages of CO_2 permeability over the range of reject flow rates considered in the analysis are displayed in Fig. 2c as a function of system pressure and CO_2 feed concentration. Larger differences between the permeability values for the 5% and the 10% CO_2 feed mixtures are obtained at lower system pressure. These differences decrease as the system pressure is raised to higher values. In addition, CO_2 permeability is higher for the

10% feed mixture than the 5% feed mixture. This behavior is a result of larger permeation driving force at higher feed pressures and increased levels of membrane plasticization caused by higher pressures and larger CO_2 content in the feed stream.

Variations in O_2 permeability as a function of feed composition, pressure, and reject flow rate are shown in Figs. 3a, 3b, and 3c. As illustrated, values of O_2 permeability vary over a wider range than CO_2. As the feed pressure is increased from 206 to 1034 kPa, O_2 permeabilities vary from low values of 2×10^{-7} to high values of 1×10^{-6} $m^3 \cdot m^{-2} \cdot s^{-1} \cdot kPa^{-1}$. For both feed compositions (Figs. 3a and 3b), O_2 permeability increases with pressure increase and decreases with an increase of the reject flow rate. This behavior is the result of a higher permeation driving force at larger system pressures. On the other hand, lower residence times caused by higher reject flow rates increase the transport resistance to permeating species.

Plasticization effects of CO_2 on variations in O_2 permeability are similar for both concentration values of CO_2 in the feed stream. This result is

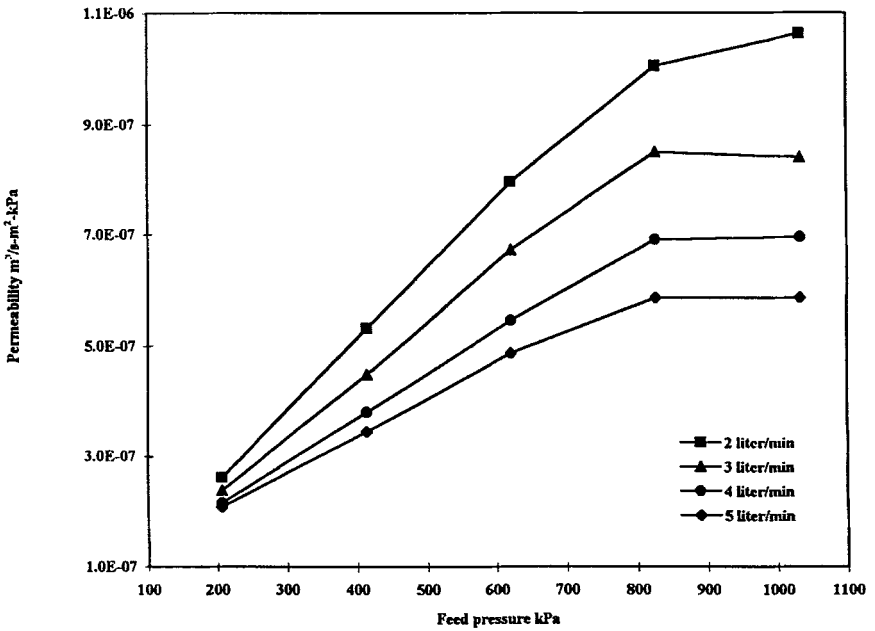

FIG. 3a Variation in O_2 permeability as a function of feed pressure and reject flow rate with a feed composition of 5% CO_2, 25% O_2, and 70% N_2.

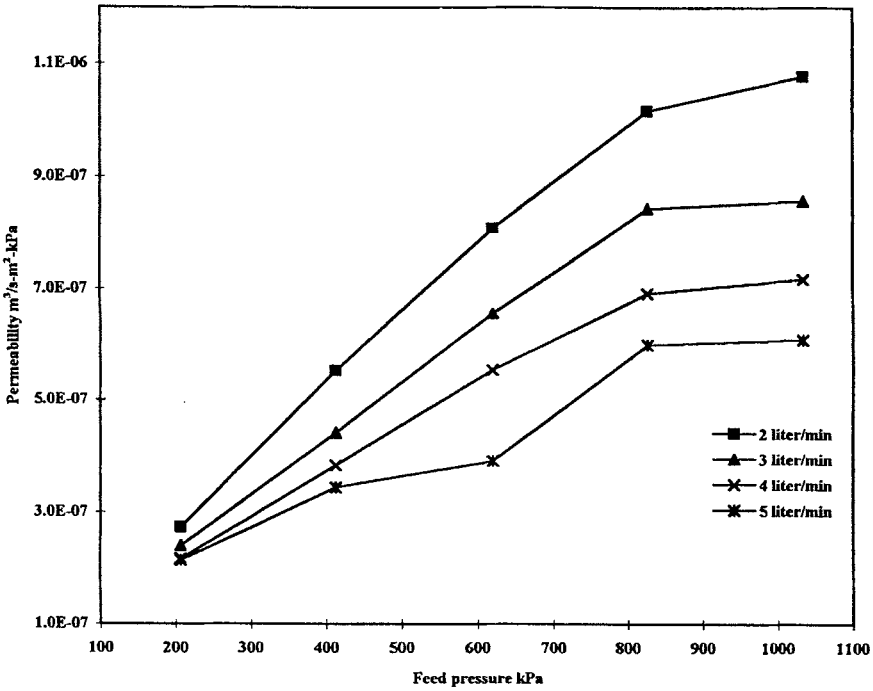

FIG. 3b Variation in O_2 permeability as a function of feed pressure and reject flow rate with a feed composition of 10% CO_2, 20% O_2, and 70% N_2.

further clarified by comparison of permeability averages for O_2 over the range of reject flow rates considered in the experiments and for both values of CO_2 concentration in the feed stream. These data are shown in Fig. 3c as are the data for variation in permeability of pure O_2. As is shown, differences between the permeability averages are negligible because of the small change in CO_2 concentration in the feed stream. On the other hand, comparisons of O_2 permeability in the gas mixture versus that of pure O_2 show large differences, especially at high pressures. This result indicates the strong effects of membrane plasticization on O_2 permeability at higher system pressures.

Permeability data for N_2 are shown in Figs. 4a, 4b, and 4c. As is shown in Figs. 4a and 4b, N_2 permeability decreases over a range of 3×10^{-8} to 5.5×10^{-8} $m^3 \cdot m^{-2} \cdot s^{-1} \cdot kPa^{-1}$ as the feed pressure is increased from 206 to 1034 kPa. In addition, variations in the reject flow rate have a

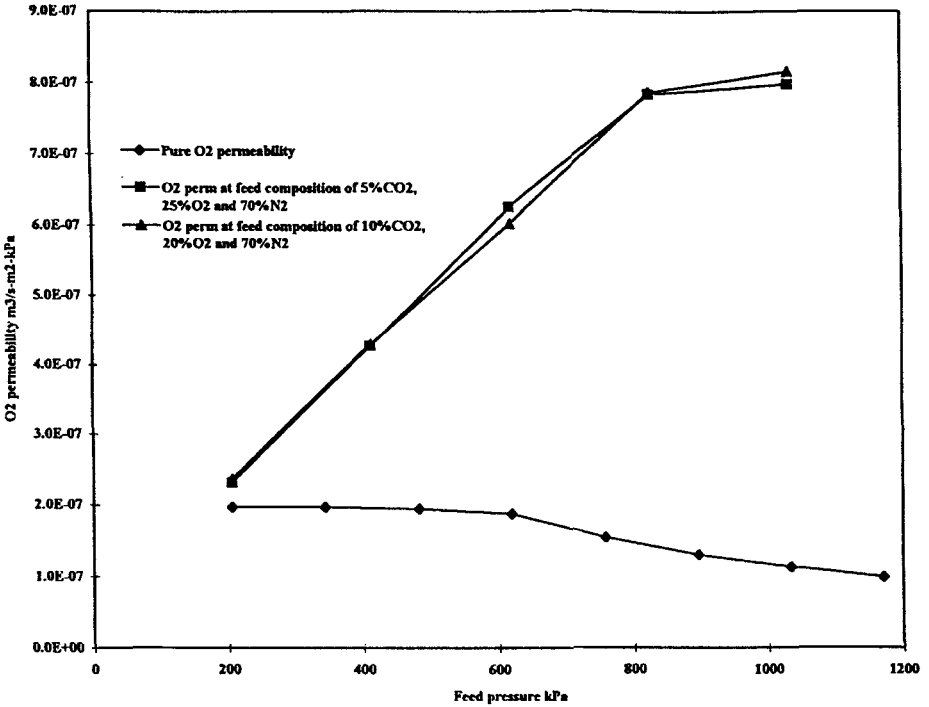

FIG. 3c Variation in average O_2 permeability as a function of feed pressure and O_2 feed concentration.

negligible effect on N_2 permeability. The decrease in N_2 permeability with pressure increase is a result of the competition among the three permeating species for adsorption sites and diffusion through the polymer chains. This competition does not favor N_2 adsorption or diffusion in comparison with the other two species. Accordingly, transport resistance encountered by N_2, which is caused by higher reject flow rates, has negligible effects on the N_2 permeation rate across the membrane.

Data in Fig. 4c show variations in averages of N_2 permeability as a function of CO_2 feed concentration and system pressure. The data for the 5 and 10 mol% CO_2 mixtures were averaged over the range of reject flow rates considered in the analysis. Results show that permeability of pure N_2 is higher than N_2 permeability in the 5 mol% CO_2 mixture. However, comparable permeabilities are obtained for pure N_2 and the 10 mol% CO_2 mixture at low system pressures. These results suggest that the level of

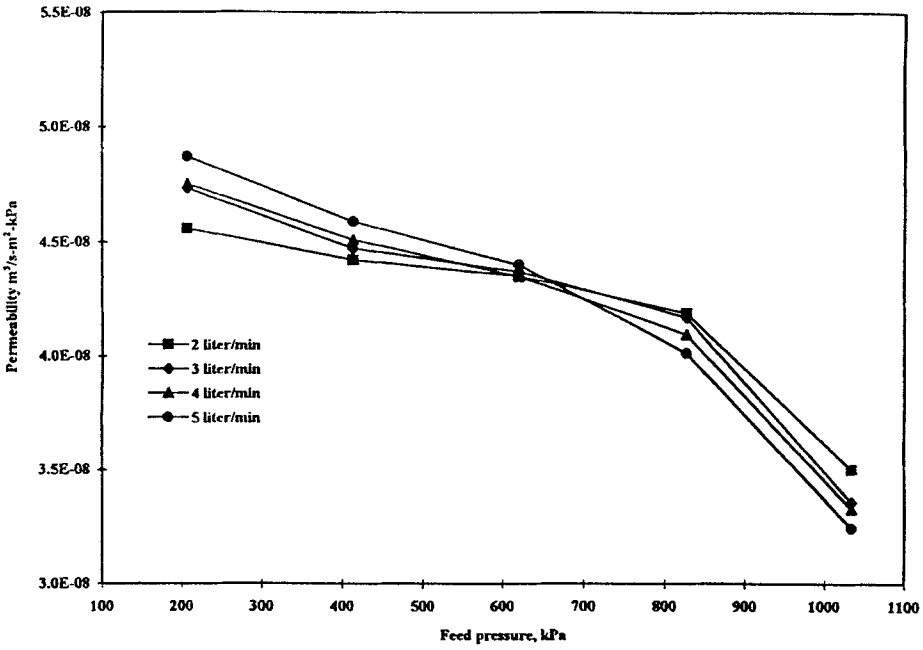

FIG. 4a Variation in N_2 permeability as a function of feed pressure and reject flow rate with a feed composition of 5% CO_2, 25% O_2, and 70% N_2.

membrane plasticization for feed mixtures of 5 and 10 mol% CO_2 are not high enough to enhance the permeability of N_2. In addition, competition among the three species favors permeation of CO_2 and O_2 more than N_2. The combined effects of species competition and the low levels of membrane plasticization with respect to N_2 result in lower N_2 permeabilities in the gas mixtures than those obtained for pure N_2.

Effects of the feed pressure, feed composition, and flow rate on species permeability are further explained in terms of the separation factors data. Figures 5a to 5c and Figs. 6a to 6c show variations in the separation factors for CO_2/N_2, CO_2/O_2, and O_2/N_2 as a function of reject flow rate, feed pressure, and feed composition. From these data it is clear that CO_2 is the fastest permeating species, followed by O_2 and then N_2.

Analysis of the separation factor data for CO_2/N_2 and CO_2/O_2 at feed mixtures of 5 and 10 mol% CO_2, which are shown in Figs. 5a, 5b, 6a, and 6b, indicate that at high system pressures the separation factor increases

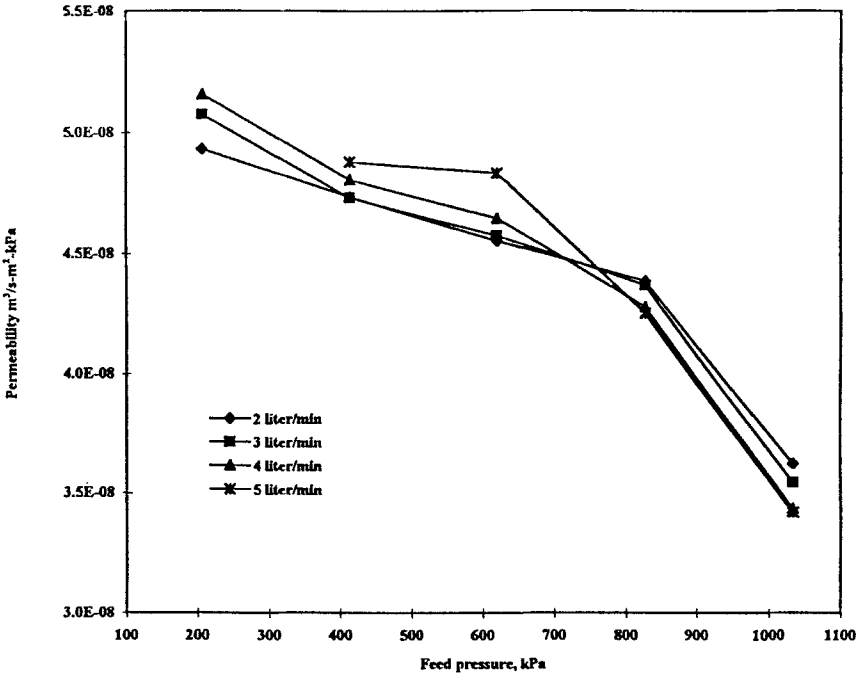

FIG. 4b Variation in N_2 permeability as a function of feed pressure and reject flow rate with a feed composition of 10% CO_2, 20% O_2, and 70% N_2.

with an increase of the reject flow rate. However, at low system pressures the separation factor decreases with an increase of the reject flow rate. As discussed before, larger system pressures result in higher levels of membrane plasticization, which enhances permeation of CO_2 versus other species. At lower system pressures, the plasticization level is limited and the effect of transport resistance caused by higher reject flow rates is more pronounced on CO_2 permeability. The pressure value at which the effect of the reject flow rate on the separation factor can be reversed is dependent on the CO_2 mol% in the feed. This behavior is clear for the separation factor data of CO_2/N_2 which are shown in Figs. 5a and 6a. In Fig. 5a, the reversed effect is realized at system pressures between 400 and 600 kPa. On the other hand and at higher CO_2 content in the feed (Fig. 6a), the reversed effect is realized at lower system pressures between 200 and 400

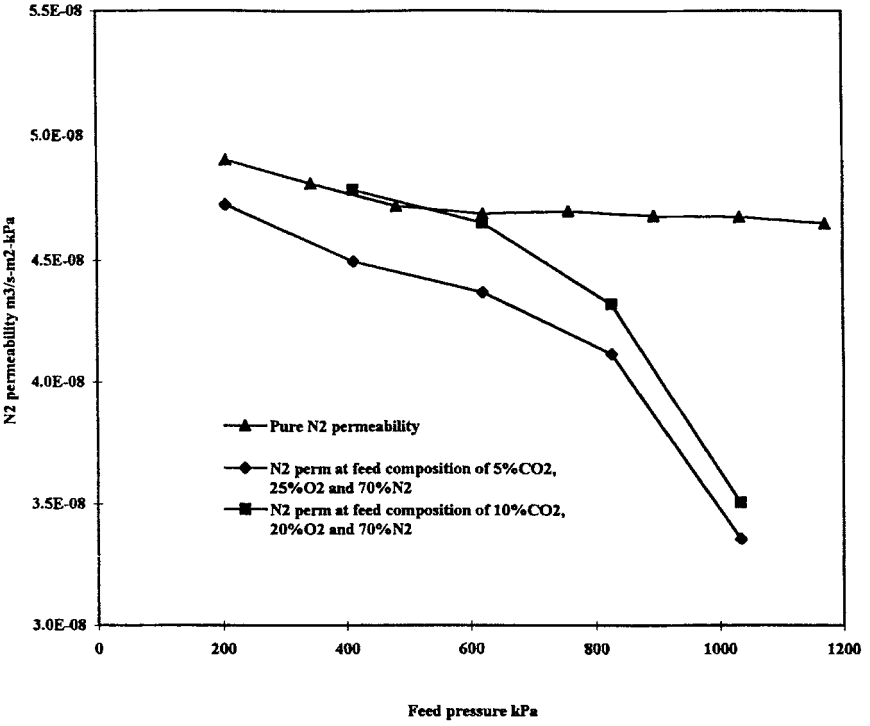

FIG. 4c Variation in N_2 permeability as a function of feed pressure and N_2 feed concentration.

kPa. The same behavior is also observed for the separation factor data of CO_2/O_2, which are shown in Figs. 5b and 6b.

Data for separation factor data of O_2/N_2 are shown in Figs. 5c and 6c as function of CO_2 content in the feed mixture, system pressure, and reject flow rate. For both sets of data the separation factor of O_2/N_2 increases with pressure increase and decrease of reject flow rate. As discussed above, higher pressures increase the driving force for permeation. On the other hand, higher reject flow rates increase the resistance for species transport within the permeator. Competition between both species favors the permeation of O_2 versus N_2 as the system pressure is increased or the reject flow rate is decreased. Increase of CO_2 content in the feed stream has a limited effect on the separation factor of O_2/N_2. This is because enhancement in permeabilities of O_2 and N_2 occur at the same level as the CO_2 feed concentration is increased.

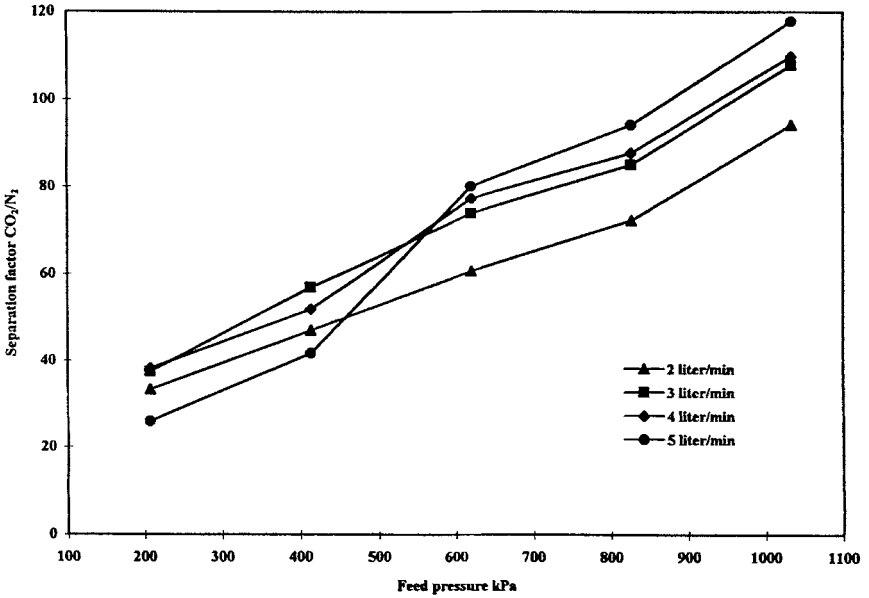

FIG. 5a Variation in separation factor CO_2/N_2 as a function of feed pressure and reject flow rate with a feed composition of 5% CO_2, 25% O_2, and 70% N_2.

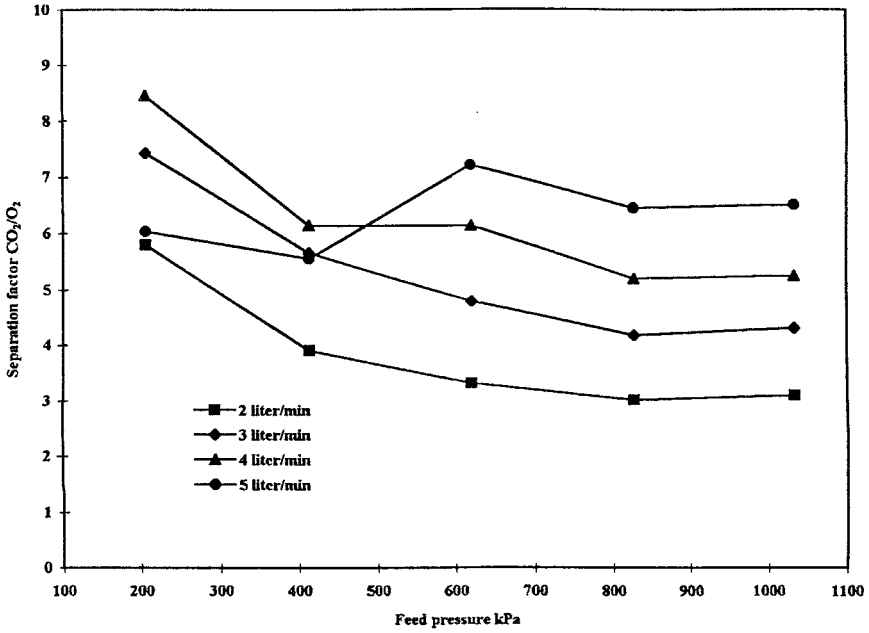

FIG. 5b Variation in separation factor CO_2/O_2 as a function of feed pressure and reject flow rate with a feed composition of 5% CO_2, 25% O_2, and 70% N_2.

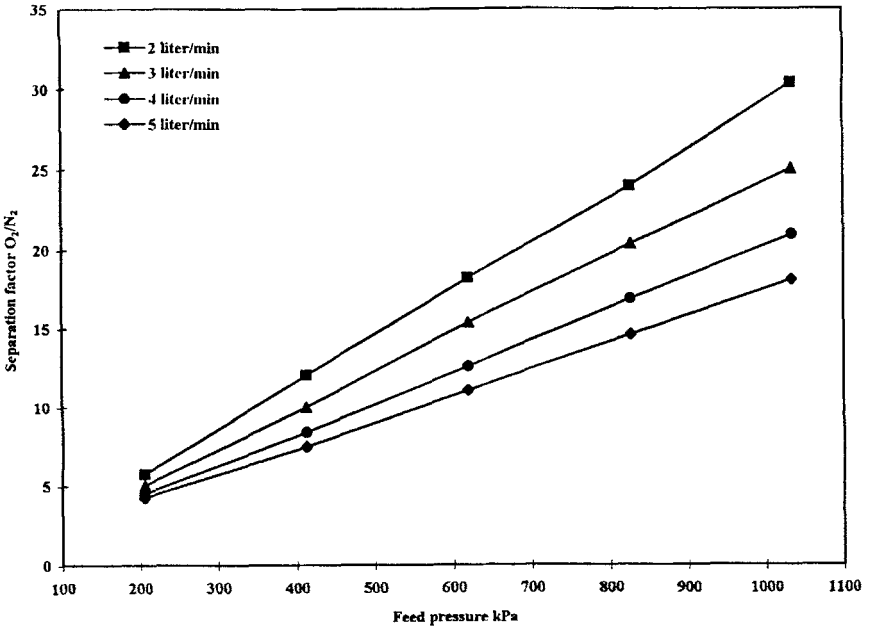

FIG. 5c Variation in separation factor O_2/N_2 as a function of feed pressure and reject flow rate with a feed composition of 5% CO_2, 25% O_2, and 70% N_2.

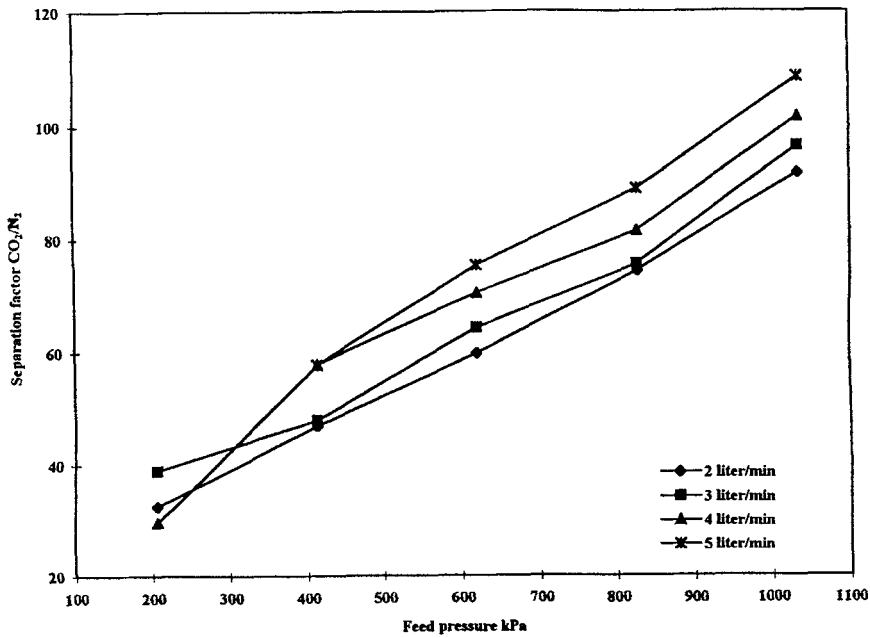

FIG. 6a Variation in separation factor CO_2/N_2 as a function of feed pressure and reject flow rate with a feed composition of 10% CO_2, 20% O_2, and 70% N_2.

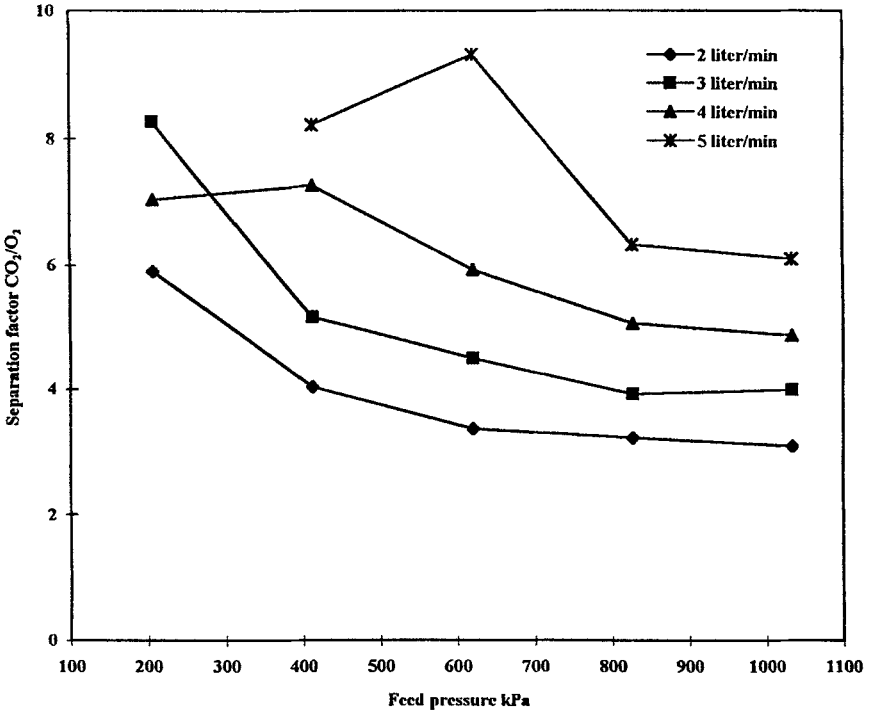

FIG. 6b Variation in separation factor CO_2/O_2 as a function of feed pressure and reject flow rate with a feed composition of 10% CO_2, 20% O_2, and 70% N_2.

Variations in the stage cut for the system as a function of the feed temperature, reject flow rate, and CO_2 feed concentration are shown in Figs. 7a and 7b. As is shown, higher system pressures and lower reject flow rates result in an increase of the stage cut. Increase of the feed pressure increases the permeation driving force and, in turn, the stage cut. On the other hand, increase of the reject flow rate reduces the residence time which increases resistance to permeation and, in turn, reduces the stage cut.

Increases of CO_2 feed concentration have a limited effect on the stage cut. For example, at a system pressure of 1034 kPa and reject flow rate of 2 $L \cdot min^{-1}$, the stage cuts are equal to 0.752 and 0.757 for feed compositions of 5 and 10 mol% CO_2, respectively. Accordingly, higher levels of membrane plasticization caused by an increase in the CO_2 content in the feed only affect the membrane selectivity.

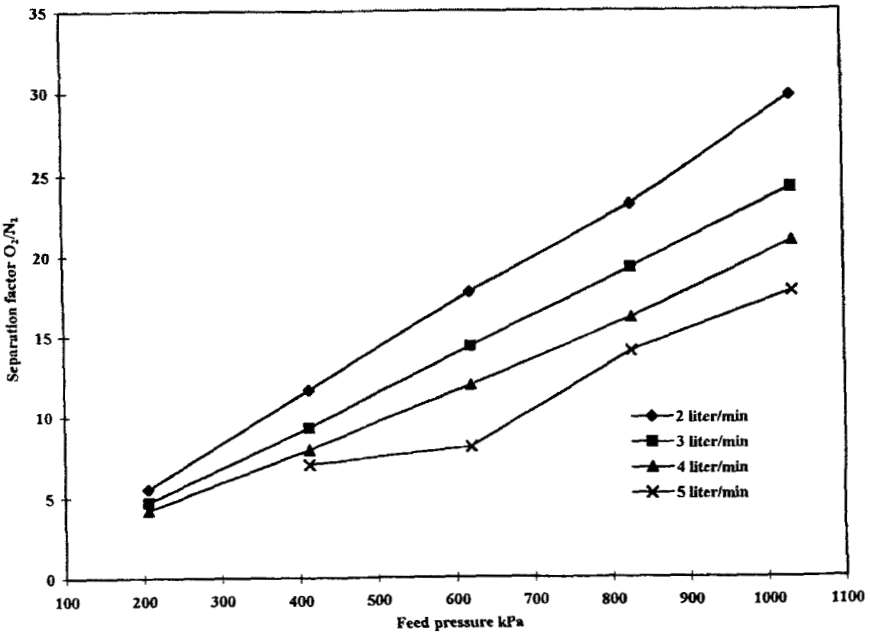

FIG. 6c Variation in separation factor O_2/N_2 as a function of feed pressure and reject flow rate with a feed composition of 10% CO_2, 20% O_2, and 70% N_2.

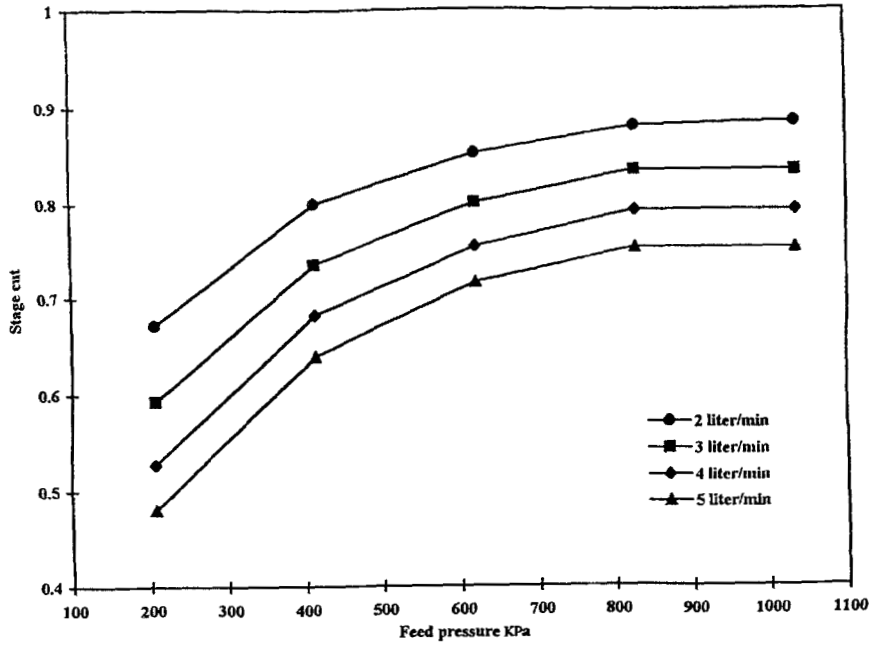

FIG. 7a Variation in stage cut as a function of feed pressure and reject flow rate with a feed composition of 5% CO_2, 25% O_2, and 70% N_2.

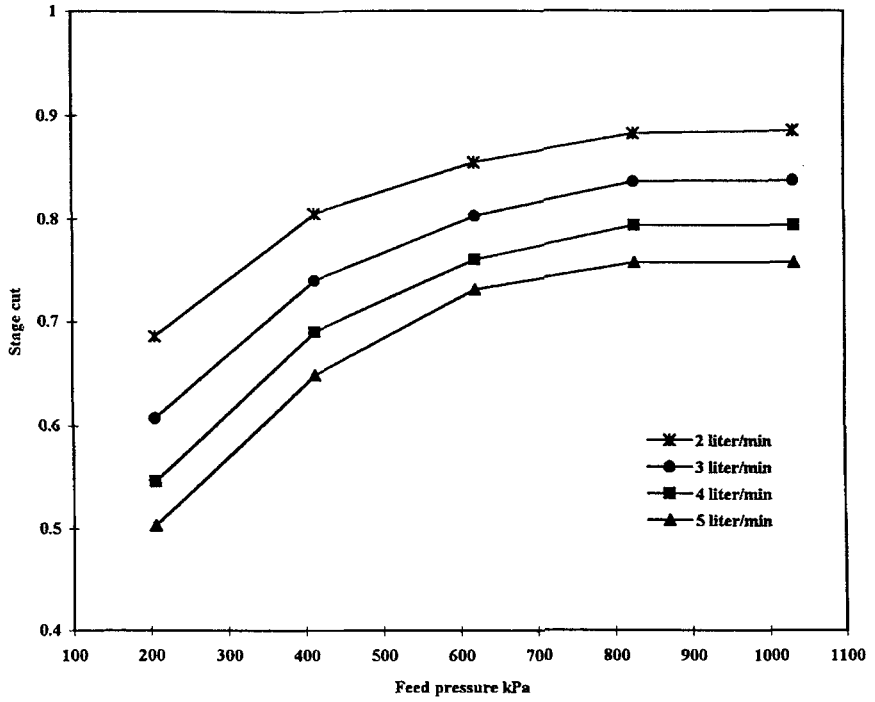

FIG. 7b Variation in stage cut as a function of feed pressure and reject flow rate with a feed composition of 10% CO_2, 20% O_2, and 70% N_2.

Results for permeate enrichment are shown in Figs. 8a and 8b. Data show that permeate enrichment has a strong dependence on system pressure and reject flow rate. On the other hand, an increase of CO_2 concentration in the feed stream has a limited effect on permeate enrichment. As illustrated in Figs. 8a and 8b, permeate enrichment increases with a decrease of the system pressure and increases of the reject flow rate. At low pressures, small levels of membrane plasticization are achieved, which result in higher membrane selectivity. In turn, CO_2 permeation rates are higher than those for O_2 and N_2, which results in higher permeate enrichment. The reverse effect is realized at higher system pressure, which, as discussed above, increases the level of membrane plasticization and enhances permeation rates for both CO_2 and O_2. The combined effects of higher reject flow rates and membrane plasticization favors CO_2 permeation against the other two species. Again, this results in higher permeate enrichment.

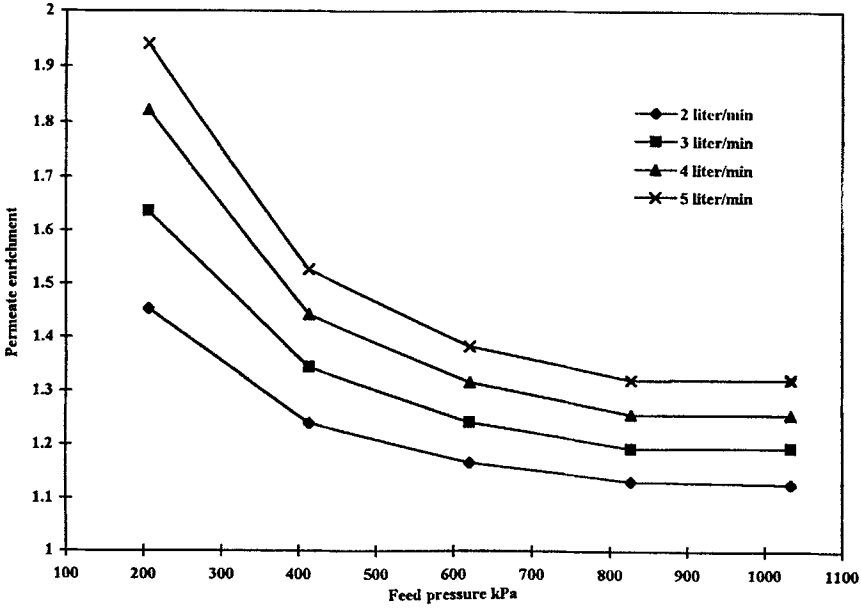

FIG. 8a Variation in permeate enrichment as a function of feed pressure and reject flow rate with a feed composition of 5% CO_2, 25% O_2, and 70% N_2.

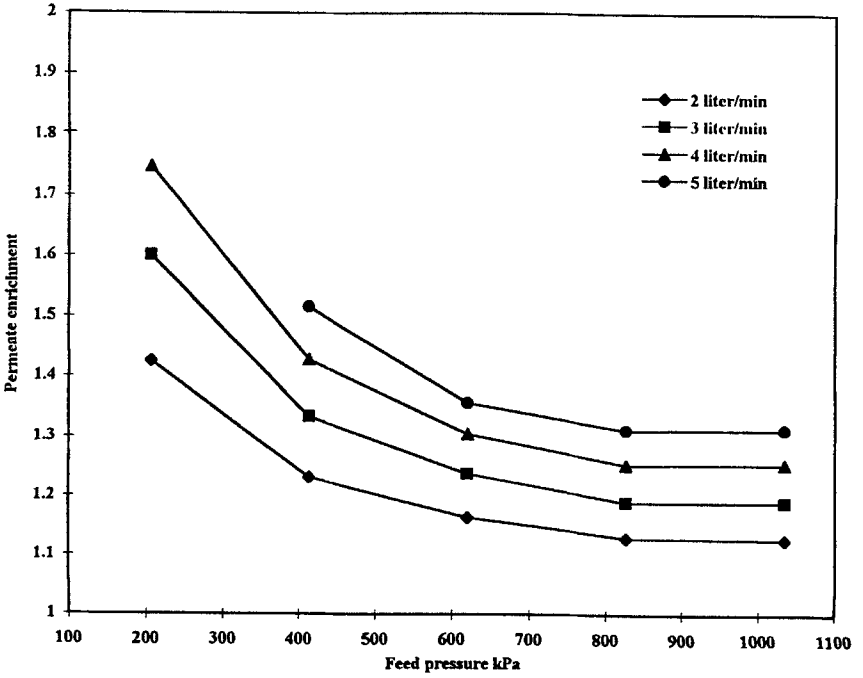

FIG. 8b Variation in permeate enrichment as a function of feed pressure and reject flow rate with a feed composition of 10% CO_2, 20% O_2, and 70% N_2.

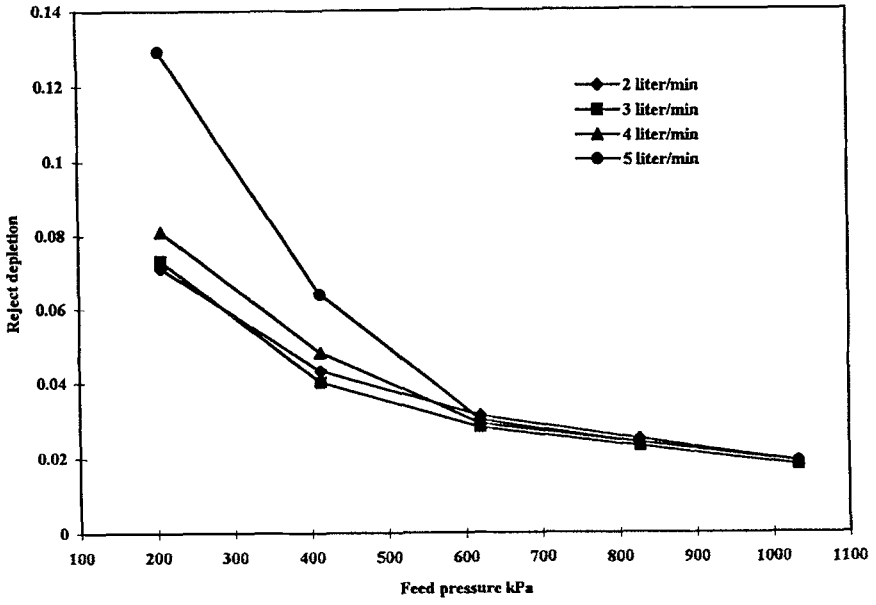

FIG. 9a Variation in reject depletion as a function of feed pressure and reject flow rate with a feed composition of 5% CO_2, 25% O_2, and 70% N_2.

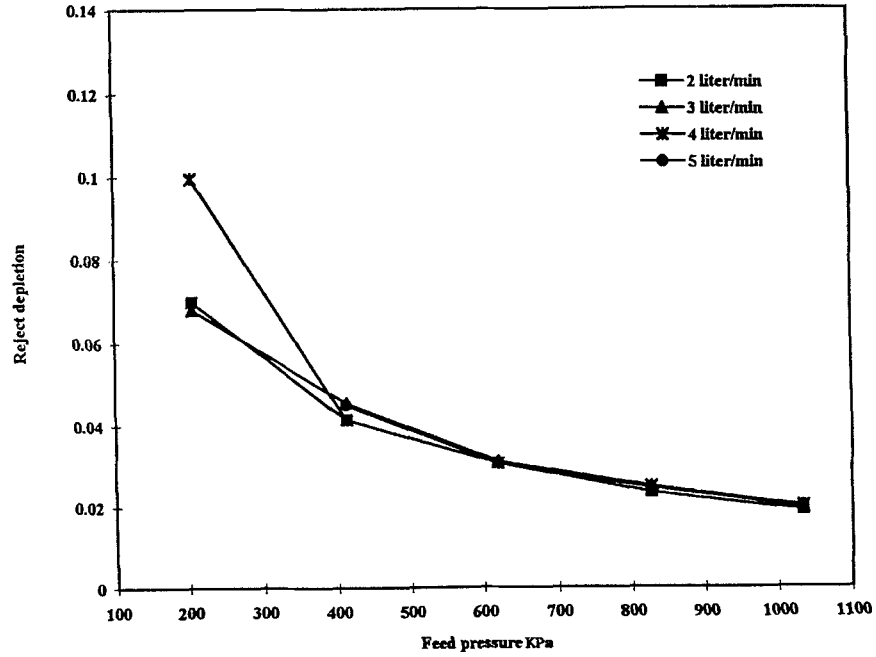

FIG. 9b Variation in reject depletion as a function of feed pressure and reject flow rate with a feed composition of 10% CO_2, 20% O_2, and 70% N_2.

Reject depletion results are shown in Figs. 9a and 9b. For all conditions considered in the analysis, reject depletion is strongly dependent on system pressure. On the other hand, much smaller effects are obtained as a function of reject flow rate and CO_2 feed concentration. As is shown in Figs. 9a and 9b, reject depletions are well below 0.1 and 0.15 for the 5% and 10% CO_2 feeds, respectively. In both cases it is clear that the majority of CO_2 in the feed stream permeates through the membrane, even at low pressures. An increase of the system pressure further reduces the reject depletion to values below 0.03 at pressures close to 1000 kPa. Accordingly, variations of reject flow rate or CO_2 feed concentrations over the range of parameters considered in this study have a very small effect on reject depletion.

CONCLUSIONS

Permeation characteristics were analyzed for a ternary system in a medium-size polysulfone hollow fiber permeator. Analysis was performed as a function of feed composition, reject flow rate, and system pressure. Reported data included species permeability, separation factors, stage cut, permeate enrichment, and reject depletion. Two feed compositions considered in the analysis included 5 and 10 mol% CO_2, 25 and 20 mol% O_2, and 70 mol% N_2.

In medium to large size permeators, transport properties affect characteristics of permeating species. In addition to resistances caused by species solution and diffusion across the membrane, transport resistances are created due to the larger size of the permeator. This effect is compounded by the presence of fast and slow permeating species in the gas mixture. The transport resistance, in addition to other permeation factors including membrane plasticization, species competition for adsorption sites, and diffusion resistance across the membrane, alters the overall permeation behavior.

Polysulfone as a glassy polymer is affected by the presence of plasticizing species such as CO_2. This results in an increase of void or hole volume between polymer chains. In turn, higher solubility and diffusion rate are achieved for permeating species. The plasticization effects reduce membrane selectivity and increase permeation flux. The degree of membrane plasticization increases with increases of the system pressure and the CO_2 content in the feed stream.

Competition between various species affects their permeation properties. For the CO_2, O_2, and N_2 gas mixture, it can be concluded that there are two levels of competition among the permeating species. The first is for CO_2 versus O_2 and N_2, and the second is between O_2 and N_2. As a result of the higher solubility and diffusion rate for CO_2, its permeability

increases with an increase of both pressure and reject flow rate. Higher pressures increases CO_2 plasticization effects and, in turn, its permeability. On the other hand, higher reject flow rates increases resistance to species transport within the permeator. The combined effect of the two factors favors the permeation of the fast species, CO_2, versus the slower species, O_2 and N_2, at higher system pressures and reject flow rates.

Stage cuts are strongly affected by the feed pressure and the reject flow rate. Higher system pressures increase the driving force for permeation across the membrane and, in turn, the stage cut. An adverse effect is obtained at higher reject flow rates which reduce the gas residence time within the permeator and, in turn, increase the transport resistance to all species within the permeator. Variations in CO_2 content in the feed have a limited effect on the stage cut. This behavior is attributed to the small range over which the CO_2 content in the feed was varied.

Permeate enrichment is strongly affected by the level of membrane plasticization and species transport resistance. Higher system pressures increase the level of membrane plasticization and, in turn, reduce membrane selectivity and permeate enrichment. An increase of the reject flow rate affects resistance to species transport within the permeator and favors CO_2 permeation versus other species. As a result, higher permeate enrichments were obtained at larger reject flow rates.

Analysis of reject depletion data show that the low content of the fast permeating species in the feed stream results in high depletion rates. As a result, reject depletion is slightly affected by system parameters which include pressure, flow rate, and composition.

ACKNOWLEDGMENT

This research is sponsored by Kuwait University Research Administration, Project EC056.

NOMENCLATURE

A	total membrane area (m^2)
P_1	feed pressure (kPa)
$\overline{P}_1$	average of feed-side pressure (kPa)
P_2	permeate pressure (kPa)
P_r	reject pressure (kPa)
Q_f	total feed flow rate ($m^3 \cdot s^{-1}$)
Q_p	total permeate flow rate ($m^3 \cdot s^{-1}$)
Q_{pi}	permeate flow rate of species i ($m^3 \cdot s^{-1}$)
Q_r	total reject flow rate ($m^3 \cdot s^{-1}$)

R_i permeability coefficient of species i ($m^3 \cdot m^{-2} \cdot s^{-1} \cdot kPa^{-1}$)
$\overline{X}_i$ average mole fraction of species i on the feed side
X_{if} mole fraction of species i in the feed stream
X_{ir} mole fraction of species i in the reject stream
y_i mole fraction of species i on the permeate side

REFERENCES

1. W. J. Koros and R. T. Chern, in *Separation of Gaseous Mixtures Using Polymer Membranes* (R. W. Rouseau, Ed.), Wiley, New York, 1987.
2. R. R. Zolandz and G. K. Fleming, "Gas Permeation," in *Membrane Handbook* (W. S. W. Ho and K. K. Sirkar, Eds.), Van Nostrand Reinhold, New York, 1992.
3. S. A. Stern and S. S. Kulkarni, "Solubility of Methane in Cellulose Acetate—Conditioning Effect of Carbon Dioxide," *J. Membr. Sci., 10*, 235–251 (1982).
4. K. Li, D. R. Acharya, and R. Hughes, "Performance of a Cellulose Acetate Permeator with Permeability-Influenced Feed," *AIChE J., 36*, 1610 (1990).
5. M. D. Donohue, B. S. Minhas, and S. Y. Lee, "Permeation Behavior of Carbon Dioxide–Methane Mixtures in Cellulose Acetate Membranes," *J. Membr. Sci., 42*, 197–214 (1989).
6. E. Sada, H. Kumazawa, P. Xu, and S. T. Wang, "Permeation of Mixed Gases in Glassy Polymer Membranes," *J. Appl. Polym. Sci., 40*, 1391–1399 (1990).
7. T. Masuda, Y. Iguchi, B. Z. Tang, and T. Higashimura, "Diffusion and Solution of Gases in Substituted Polyacetylene Membranes," *Polymer, 29*, 2041–2049 (1988).
8. N. Cao, M. Pegoraro, F. Bianchi, L. D. Landro, and L. Zanderighi, "Gas Transport Properties of Polycarbonate–Polyurethane Membranes," *J. Appl. Polym. Sci., 48*, 1831–1842 (1993).
9. E. Staude and L. Breitbach, "Polysulfones and Their Derivatives: Materials for Membranes for Different Separation Operations," *Ibid., 43*, 559–566 (1991).
10. J. A. Barrie and M. J. L. Williams, "Gas Transport in Heterogeneous Polymer Blends," *J. Membr. Sci., 21*, 185–202 (1984).
11. J. A. Barrie and W. D. Webb, "Gas Transport in Miscible Blends of Ethylene Vinyl Acetate Copolymer and Chlorinated Polyethylene," *Polymer, 30*, 327–332 (1989).
12. M. R. Coleman, R. Kohn, and W. J. Koros, "Gas-Separation Applications of Miscible Blends of Isomeric Polyimides," *J. Appl. Polym. Sci., 50*, 1059–1064 (1993).
13. G. Morel and D. R. Paul, "CO_2 Sorption and Transport in Miscible Poly(Phenylene Oxide)/Polystyrene Blends, *J. Membr. Sci., 10*, 273–282 (1982).
14. P. H. Pfromm, I. Pinnau, and W. J. Koros, "Gas Transport through Integral-Asymmetric Membranes: A Comparison to Isotropic Film Transport Properties," *J. Appl. Polym. Sci., 48*, 2161 (1993).
15. E. Sada, H. Kumazawa, Y. Yoshio, S.-T. Wang, and P. Xu, "Permeation of Carbon Dioxide through Homogeneous Dense and Asymmetric Cellulose Acetate Membranes," *J. Polym. Sci., 26*, 1035 (1988).
16. J. D. Le Rous, D. R. Paul, J. Kampa, and R. J. Lagow, "Modification of Asymmetric Polysulfone Membranes by Mild Surface Flourination," *J. Membr. Sci., 94*, 121–141 (1994).

Received by editor July 26, 1995